

UNCLASSIFIED

AD

AD-E404 268

Technical Report ARMET-TR-19007

THREE-DIMENSIONAL PRINTED YAWSONDE SOLAR SENSOR

Aaron Barton
Vincent Cascella
Delfin Quijano
Joshua Kulik
Matt Clemente

January 2021



U.S. ARMY COMBAT CAPABILITIES DEVELOPMENT
COMMAND ARMAMENTS CENTER

Munitions Engineering Technology Center

Picatinny Arsenal, New Jersey

Approved for public release; distribution is unlimited.

UNCLASSIFIED

UNCLASSIFIED

The views, opinions, and/or findings contained in this report are those of the author(s) and should not be construed as an official Department of the Army position, policy, or decision, unless so designated by other documentation.

The citation in this report of the names of commercial firms or commercially available products or services does not constitute official endorsement by or approval of the U.S. Government.

Destroy by any means possible to prevent disclosure of contents or reconstruction of the document. Do not return to the originator.

UNCLASSIFIED

UNCLASSIFIED

REPORT DOCUMENTATION PAGE			<i>Form Approved</i> <i>OMB No. 0704-01-0188</i>		
<p>The public reporting burden for this collection of information is estimated to average 1 hour per response, including the time for reviewing instructions, searching existing data sources, gathering and maintaining the data needed, and completing and reviewing the collection of information. Send comments regarding this burden estimate or any other aspect of this collection of information, including suggestions for reducing the burden to Department of Defense, Washington Headquarters Services Directorate for Information Operations and Reports (0704-0188), 1215 Jefferson Davis Highway, Suite 1204, Arlington, VA 22202-4302. Respondents should be aware that notwithstanding any other provision of law, no person shall be subject to any penalty for failing to comply with a collection of information if it does not display a currently valid OMB control number.</p> <p>PLEASE DO NOT RETURN YOUR FORM TO THE ABOVE ADDRESS.</p>					
1. REPORT DATE (DD-MM-YYYY) January 2021		2. REPORT TYPE Final		3. DATES COVERED (<i>From - To</i>) November 2017 to June 2018	
4. TITLE AND SUBTITLE Three-dimensional Printed Yawsonde Solar Sensor			5a. CONTRACT NUMBER		
			5b. GRANT NUMBER		
			5c. PROGRAM ELEMENT NUMBER		
6. AUTHORS Aaron Barton, Vincent Cascella, Delfin Quijano, Joshua Kulik, and Matt Clemente			5d. PROJECT NUMBER		
			5e. TASK NUMBER		
			5f. WORK UNIT NUMBER		
7. PERFORMING ORGANIZATION NAME(S) AND ADDRESS(ES) U.S. Army DEVCOM AC, METC Fuze & Precision Armaments Technology Directorate (FCDD-ACM-FI) Picatinny Arsenal, NJ 07806-5000			8. PERFORMING ORGANIZATION REPORT NUMBER		
9. SPONSORING/MONITORING AGENCY NAME(S) AND ADDRESS(ES) U.S. Army DEVCOM AC, ESIC Knowledge & Process Management Office (FCDD-ACE-K) Picatinny Arsenal, NJ 07806-5000			10. SPONSOR/MONITOR'S ACRONYM(S)		
			11. SPONSOR/MONITOR'S REPORT NUMBER(S) Technical Report ARMET-TR-19007		
12. DISTRIBUTION/AVAILABILITY STATEMENT Approved for public release; distribution is unlimited.					
13. SUPPLEMENTARY NOTES					
14. ABSTRACT This report describes a three-dimensional printed solar sensor for use as a part of a yawsonde, a device for measuring flight dynamics of spinning projectiles. The sensor is fabricated using additive manufacturing, making it fast and inexpensive to produce. The sensor incorporates light-trapping ridge features printed directly into the housing, which previously needed to be machined into the sensor body. The sensor was fabricated in plastic using stereolithography, and in metal using selective laser sintering.					
15. SUBJECT TERMS Telemetry Instrumentation High-g Gun launched Munitions Aeroballistics Diagnostic fuze DFuze Aeroballistics fuze Aerofuze Yawsonde Solar sensor Solar likeness indicating transducer ARL SLIT Additive manufacturing 3D printing Stereolithography Selective laser sintering					
16. SECURITY CLASSIFICATION OF:			17. LIMITATION OF ABSTRACT	18. NUMBER OF PAGES	19a. NAME OF RESPONSIBLE PERSON
a. REPORT	b. ABSTRACT	c. THIS PAGE			Aaron E. Barton
U	U	U	SAR	27	19b. TELEPHONE NUMBER (Include area code)

CONTENTS

	Page
Introduction	1
Prior Art	1
Yawsonde Theoretical Field of View	5
Three-dimensional Printed Yawsonde	7
Sensor Output Comparison	15
Conclusions	18
References	19
Distribution List	21

FIGURES

1 BRL yawsonde solar sensor	2
2 BRL yawsonde	3
3 ARL SLIT solar sensor - three-dimensional (3D) rendering	4
4 ARL SLIT solar sensor - mounted to fuze	4
5 Peak roll location for a 30-deg tilted solar sensor on a circular cylinder	5
6 Peak roll location for a 30-deg tilted solar sensor on a 10-deg slanted cone	6
7 Rendering of peak roll location loci on the spherical field of view of a two yawsonde system	7
8 Renderings of the 3D-printed yawsonde	8
9 Plastic 3D-printed solar sensor	9
10 Plastic 3D-printed solar sensors mounted on fuze housing	10
11 Plastic 3D-printed solar sensors mounted on fuze - up close view	11
12 Two-piece metal clamshell 3D printed solar sensor with scale removed	12
13 Single-piece metal (with scale) 3D-printed solar sensor: top - front/bottom - rear	13
14 3D-printed solar sensor slit comparison: top - single-piece metal with scale/bottom - single-piece plastic	14
15 Two-piece scaled clamshell metal 3D-printed solar sensor	14
16 Solar sensor calibration table	15

UNCLASSIFIED

FIGURES
(continued)

	Page
17 Schematic for solar sensor signal conditioning printed circuit board (P/N DEVCOM AC 0610-00424 AMM085-SS)	16
18 Comparison of plastic 3D solar sensor and ARL SLIT solar sensor signal outputs: left - unsaturated/right - saturated	17
19 Plastic 3D-printed yawsonde output on a rotating fuze for solar aspect angles 40 to 130 deg	17
20 ARL SLIT sensor on a rotating fuze for solar aspect angles 30 to 140 deg	18

UNCLASSIFIED

ACKNOWLEDGMENTS

The authors would like to thank Ductri Nguyen for assistance in obtaining funding for this work as a part of the Extended Range Cannon Artillery program, Pavol Stofko for mechanical support, Mike Hollis for his help in using solar sensors over the years, Jacob Struck for his work in building a solar table calibrator on previous programs, Stephan Zuber and James Hitscherich for their optical engineering support, and Bradford Davis for reviewing this report and providing background information on solar sensor design and usage. They would also like to thank the Precision Munitions Instrumentation Division staff for their support.

UNCLASSIFIED

INTRODUCTION

Solar sensors have enjoyed a rich history of usage on yawsondes for U.S. Army munitions programs. A yawsonde is a device used to measure the flight dynamics of spinning projectiles, including spin and attitude estimates. Solar sensors are employed within these devices to estimate projectile orientation, using the sun as a reference. These sensors typically consist of a photodiode placed within a housing that has a small slit or pinhole aperture. This casts sunlight on the photodiode, in such a way that the voltage or current output varies with changes in the angle between the projectile spin axis and the direction to the sun. This is referred to in literature as the solar aspect angle σ_s . As the projectile spins, the sunlight incident on the photodiode creates a pulse position modulated electrical pulse train, with the time between pulses depending on the solar aspect angle. The electrical pulse train is then telemetered, recorded, and processed to obtain a graph of the solar aspect angle during muzzle exit and during flight.

Other sensors have been used on yawsondes to measure projectile dynamics such as micro-electro-mechanical systems (MEMS) magnetometers, accelerometers, and gyroscopes. However, these sensors have been shown to have gun-launched and platform-induced effects that makes accurate projectile measurements difficult, including distortion of the geomagnetic field by the projectile body and shock-induced bias and gain shifts. Solar sensors, being entirely optical devices, have been shown to be immune to such effects. They have been treated as a gold standard for evaluating measurements from other sensors as well as correcting those measurements using sensor fusion algorithms (refs. 1 through 3).

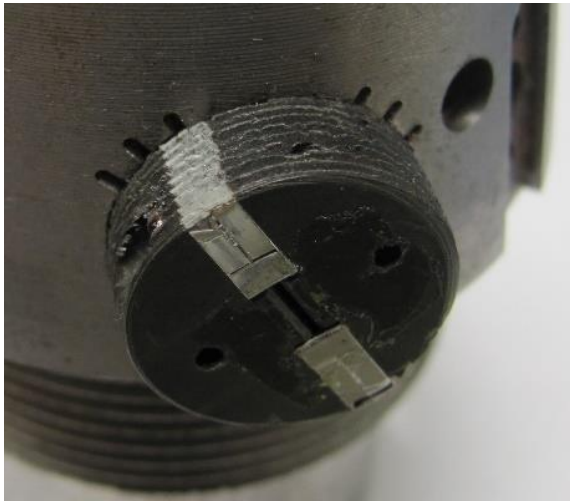
An important limitation in using solar sensors is that the projectile must be fired during the day, within a certain time window where the sun is within view and near-perpendicular to the sensor, and with minimal cloud coverage. The time window changes for different firing angles. This limitation has precluded solar sensor for tactical use, which requires all-weather day and night capability.

PRIOR ART

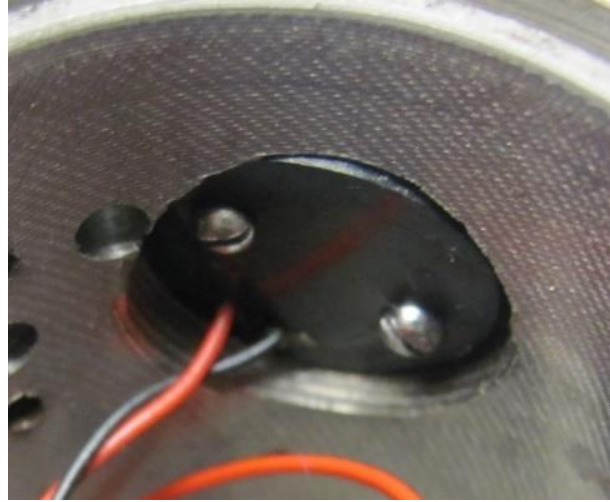
Designs for solar sensors date back to the late 1960s for the High Altitude Research Project (ref. 4). Development since this time occurred due to the efforts of personnel from the former Ballistic Research Laboratories (BRL), Aberdeen Proving Ground, MD, former Harry Diamond Laboratories (HDL), Adelphi, MD, U.S. Army Research Laboratories (ARL), Adelphi, MD, and divisions at the U.S. Army Combat Capabilities Development Command Armaments Center (DEVCOM AC), Picatinny Arsenal, NJ. Early designs include pinhole yawsondes, credited to development at HDL and referred to in literature as the "HDL yawsonde" (refs. 5 through 8). These designs feature an instrumented standard artillery fuze with a small pinhole. Within the fuze is a photodiode (or photodiode array), covered with an optical masking with two or more slits in the shape of the letter "V." As the projectile spins, light from the pinhole transverses the legs of the "V," generating a series of pulses whose duty cycle depends on solar aspect angle. Pinhole yawsondes sensors typically required a large intrusion into the instrumented fuze in order to accommodate the space between the aperture and optical mask.

Engineers at the BRL and DEVCOM AC later developed another yawsonde—referred to in literature as the "Short Intrusion" or "BRL" yawsonde—which does away with the pinhole and optical mask. Instead, as shown in figure 1, each photodiode is housed in a separate sensor, featuring a round plastic housing that contains a slit, serrated walls acting as light traps, and reflectors (refs. 4 and 9 through 12). This slit allows sunlight to penetrate to the photodiode only when it crosses along its plane. Shown in figure 2, the solar sensor screws into the side of the fuze housing and is clocked so that the slit axis is at an adjustable angle with the projectile main axis. Two or more sensors placed around the perimeter of the fuze, with several tilted, create the same effect as the "V" slots in

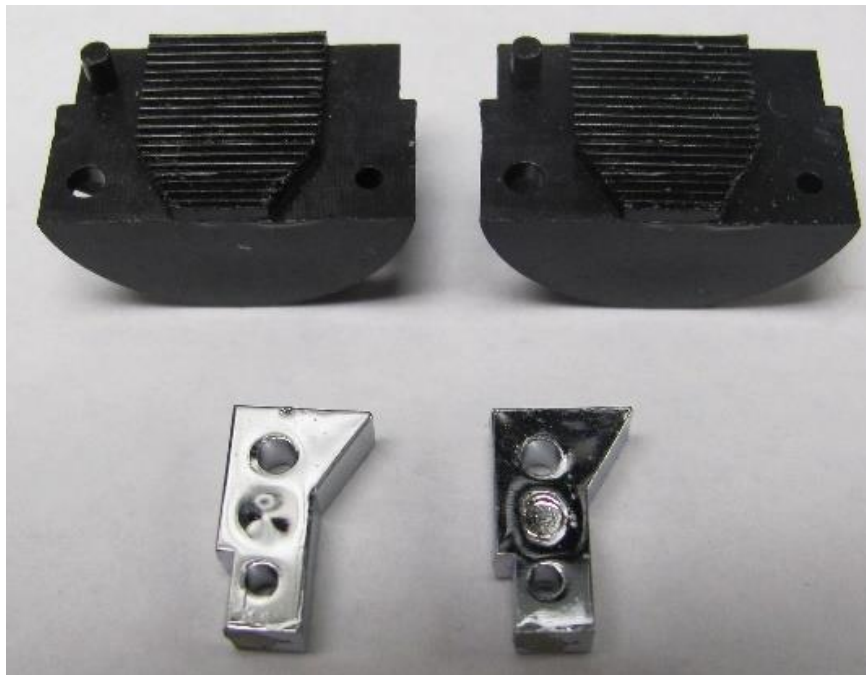
the HDL pinhole yawsonde. As the projectile spins, the sensors generate a series of pulses, the duty cycle of which depends on solar aspect angle.



(a)
Exterior



(b)
Interior



(c)
Parts

Figure 1
BRL yawsonde solar sensor



Figure 2
BRL yawsonde

Engineers at the ARL later improved on this design to reduce intrusion by using a smaller machined-aluminum two-piece shroud with an optical slit (ref. 13); this was known as the Jet Propulsion Laboratory Free Flying Magnetometer (JPL-FFM) solar sensor. The geometry of the sensor was refined, and this sensor was later referred to as the ARL solar light indicating transducer (SLIT), which is the current state of the art model. Further improvement by the ARL led to the aeroballistic diagnostic fuze (DFuze), which combined the SLITs with magnetometers, gyroscopes, magnetometers, low-g accelerometers, and high-g accelerometers (refs. 14 and 15).

The ARL SLIT sensor consists of a two-piece, precision-machined aluminum clamshell shroud. Similar to the BRL yawsonde solar sensor, there are light-absorbing ridges on the sides of the slit, machined into the aluminum, which act to eliminate reflections on the inner sidewalls, narrowing the angle of acceptance of the sensor and reducing the pulse width. Obstructing pillars act to reduce light intensity when the sensor is directly pointed at the sun. Parabolic reflectors act to guide light from the far-off angle, increasing the angle of acceptance in the plane of the slit. A 3D rendering of these sensors is shown in figure 3. These sensors are press-fit into tilted slots on the fuze housing, as shown in figure 4. As the projectile spins, the sensors generate a series of pulses whose duty cycle depends on solar aspect angle—the same effect as the BRL yawsonde solar sensor.

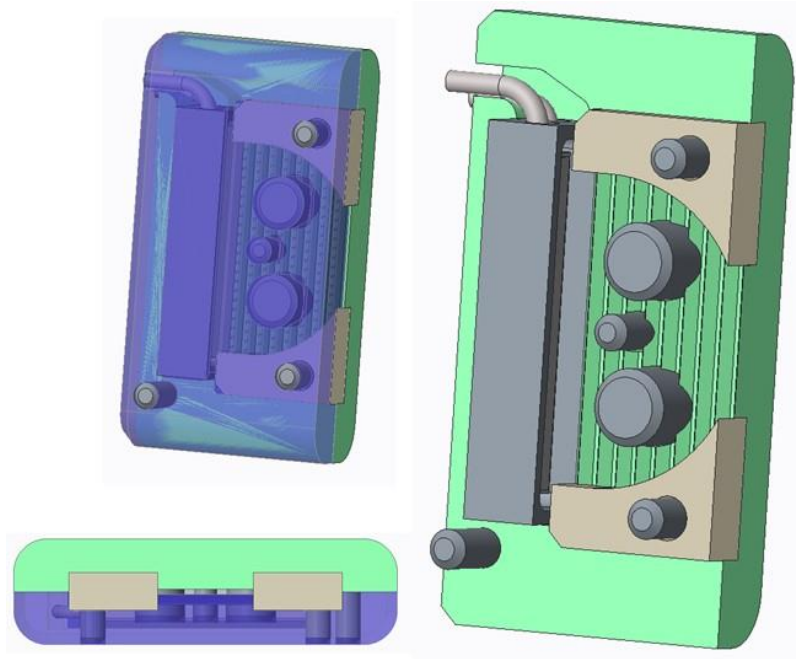


Figure 3
ARL SLIT solar sensor - three-dimensional (3D) rendering

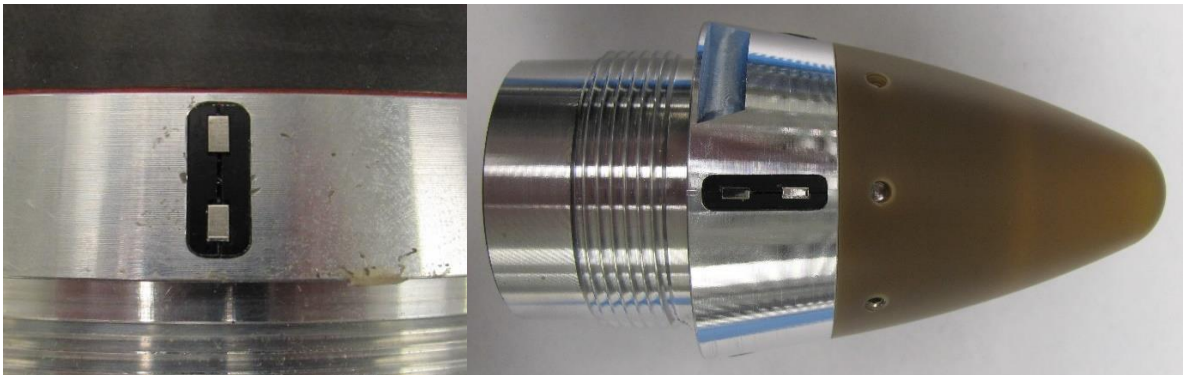


Figure 4
ARL SLIT solar sensor - mounted to fuze

The additional design details can be found in reference 16. An analysis of the sensor design using Zemax optical design software can be found in reference 17. This was performed in conjunction with the additive manufacturing effort of this report.

Other markets for solar sensors include attitude control on spacecraft. Recent sensors are designed for attitude and spin measurements on CubeSats, which prioritize low size, cost, and weight, including SolarMEMS (refs. 18 and 19). These sensors could be used on spin-stabilized projectiles, as long as they could be proven to survive high-g shock environments and function in the high spin (greater than 200 Hz) seen on such platforms.

YAWSONDE THEORETICAL FIELD OF VIEW

A set of solar sensors, placed on the outer perimeter of a spinning projectile, will output a series of pulses as the sun passes over each sensor's field of view. With one sensor tilted at an angle (typically 30 deg in practice), the pulse position changes with the solar aspect angle. For a single solar sensor placed on a cylinder—such as on the sidewall of a projectile body—the formula for the roll angle location of the pulse peak is given in reference 13, and is repeated in equation 1.

$$\phi = \phi_o - \sin^{-1} \left(\frac{\tan(\gamma)}{\tan(\sigma_s)} \right) \quad (1)$$

Where ϕ_o is the circumferential location of the sensor, γ is the sensor tilt angle from vertical, and σ_s is the solar aspect angle. This function is plotted in figure 5 for $\phi_o = 90 \text{ deg}$, $\gamma = 30 \text{ deg}$. Note that the peak roll location is directly over the sensor at $\phi = 90 \text{ deg}$, when the solar aspect angle $\sigma_s = 90 \text{ deg}$, which is when the sun is at the sensor's zenith.

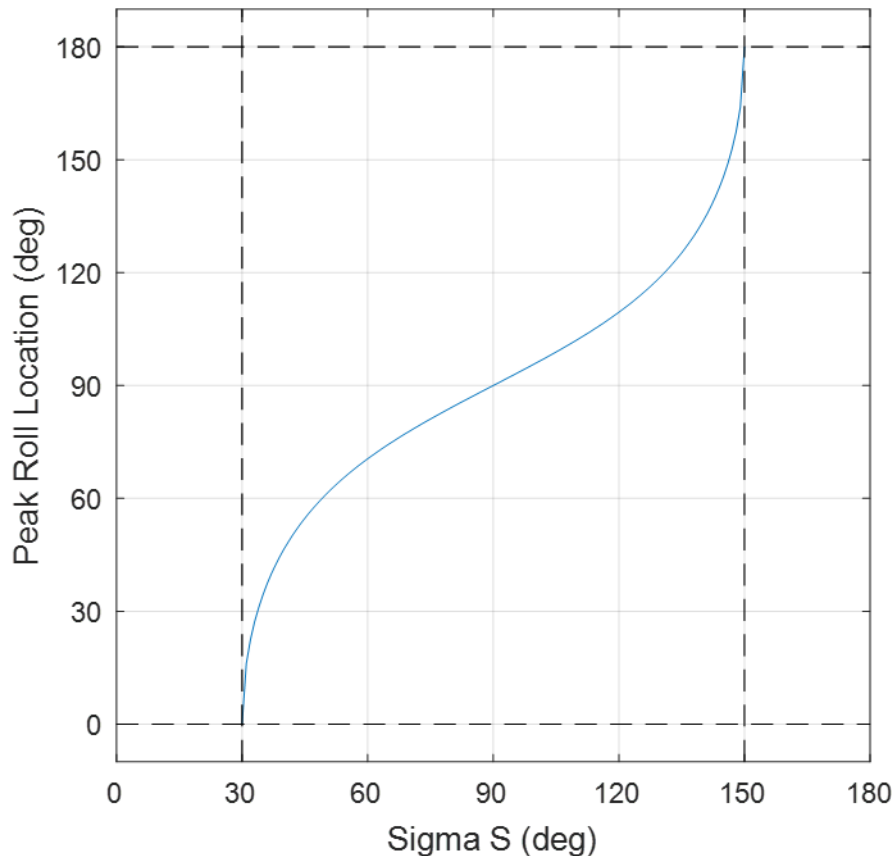


Figure 5
Peak roll location for a 30-deg tilted solar sensor on a circular cylinder

If the solar sensor is placed on a conical section instead of a cylinder, such as on a projectile or fuze ogive section, the formula, as shown in equation 2, is slightly different.

$$\phi = \phi_o - \sin^{-1} \left(\frac{\tan(\gamma)}{\tan(\sigma_s + \tau) \cos(\tau) - \sin(\tau)} \right) \quad (2)$$

Where τ is the inward tilt angle of the cone wall from vertical. For $\phi_o = 90 \text{ deg}$, $\gamma = 30 \text{ deg}$, and $\tau = 10 \text{ deg}$, the function is plotted in figure 6. Note that the peak roll location is directly over the sensor at $\phi = 90 \text{ deg}$, when the solar aspect angle $\sigma_s = 80 \text{ deg}$, which is when the sun is at the sensor's zenith on the cone.

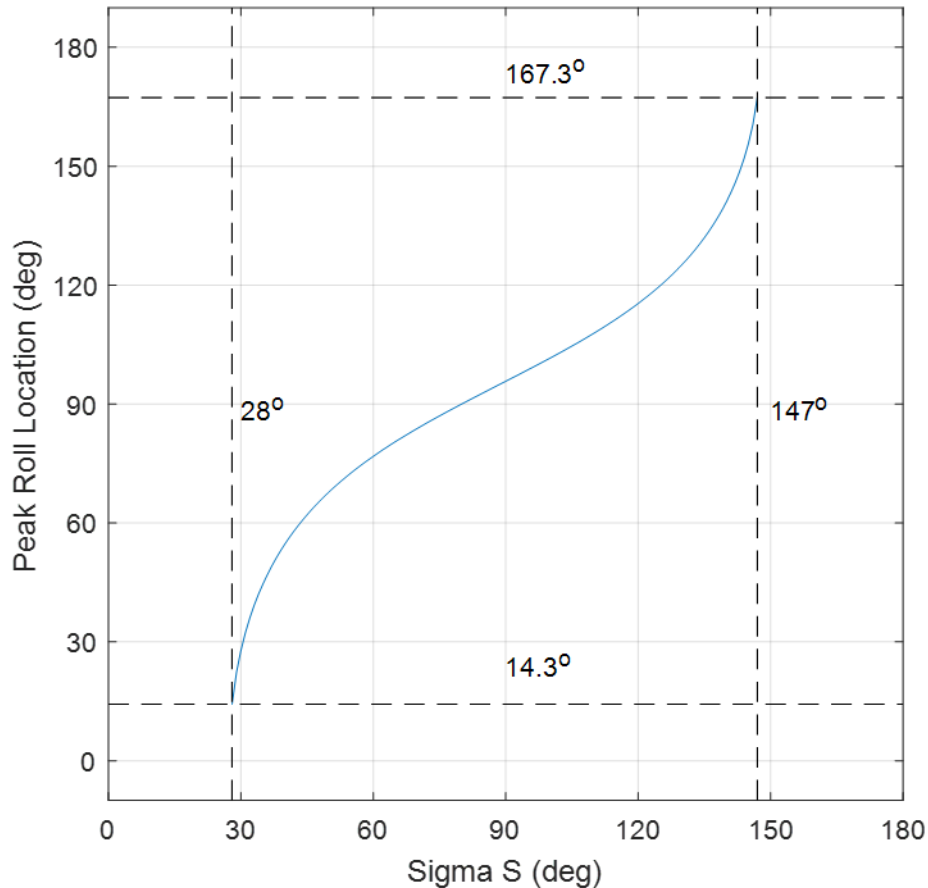


Figure 6
Peak roll location for a 30-deg tilted solar sensor on a 10-deg slanted cone

The equations show that there is a maximum range for the solar aspect angle measurement. This is regardless of the field of view of the individual sensor. For two solar sensors, where one is arranged vertically and one tilted, the end of the range corresponds to the roll angle where the pulses from the vertical and tilted sensors coincide. This is shown in figure 7. The sphere represents the field of view of the projectile in spherical coordinates. The vertical black line on the sphere represents the field of view midline of a vertical sensor, and the tilted red line represents the field of view midline of a tilted sensor. The sensors are 90 deg apart and are placed on a cylinder.

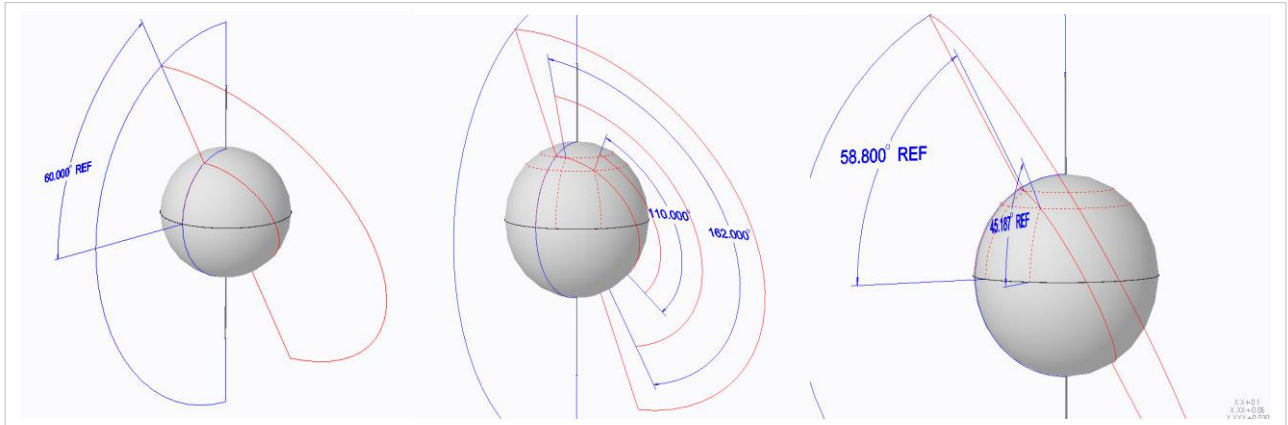


Figure 7

Rendering of peak roll location loci on the spherical field of view of a two yawsonde system

For solar sensors with perfect 180-deg fields of view, the black lines and red lines coincide at elevation angles of 60 deg, which agrees with equation 1. Therefore, to create a solar sensor pair for a greater than +/-60-deg functionality requires lowering the sensor tilt angle γ , while ensuring the sensor field of view is as close as possible to 180 deg. The former will involve the reducing of system sensitivity, as the pulse timings will become less sensitive to the solar aspect angle. The latter involves using large height solar sensors or sensors with built-in reflectors. Sidewall reflectors are what allow for a wide field of view in the BRL and ARL SLIT yawsonde designs.

It is possible to reduce the sensor field of view without sacrificing much of the yawsonde system operating range. The ARL SLIT sensor field of view was analyzed as +/-81 deg in reference 17, and this allows for a two-sensor (one vertical, one tilted with $\gamma = 30 \text{ deg}$) system range of +/-58.8 deg, which is 98% of the full coverage of the total theoretical +/-60 deg available. If the sensor field of view was reduced to +/-55 deg, the system field of view becomes +/-45.1 deg, as shown previously in figure 7. This is still 75% of the full theoretical +/-60-deg coverage available. If the projectile yawing motion to be measured is expected to be within this range, and if the projectile is fired at a time where the sun is perpendicular to the sensor face, then this range is acceptable.

THREE-DIMENSIONAL PRINTED YAWSONDE

Tight tolerance, multiple machined parts requiring multiple hand assembly steps have usually made each ARL SLIT sensor a high-cost, long-lead item. Modern additive manufacturing allows for the rapid fabrication of custom parts, including internal mechanical features that could be created by conventional machining. Solar sensor shrouds with light traps and obstrucater features can be printed at low cost, with short lead time, and requiring significantly fewer assembly steps.

The 3D printed yawsonde solar sensor consists of a single piece 3D printed body with a flattened inverted cone shaped optical slit that includes side wall light-trapping ridges printed directly into it. Computer-aided drawing renderings are shown in figure 8. The slit acts as a light pipe to an inexpensive 3-mm T-1 packaged, flat-headed, wide-angle photodiode, which is inserted into the back of the shroud in a small pocket and is epoxy sealed in place. The slit angle is designed for a +/- 55-deg field of view on the insensitive axis. While this is less than the ARL SLIT sensor, the resulting system range is still acceptable for capturing projectile motion for most ballistic tests. The outer profile of the sensor was designed to match the ARL SLIT sensor. The slit can optionally be filled with a clear casting resin. The resin creates refraction on the surface of the slit, acting as a small lens, to increase the angle of acceptance along the slit plane, at the expense of a slight increase along the sensitive axis. Two versions of this sensor were developed by two additive manufacturing branches at the DEVCOM AC: one in plastic using stereo-lithography, another in metal using selective laser sintering.

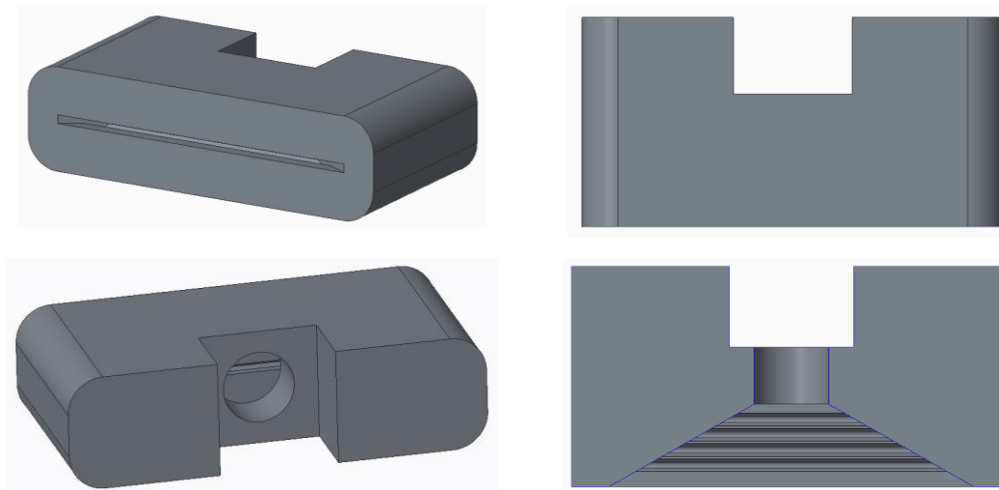


Figure 8
Renderings of the 3D-printed yawsonde

The plastic sensors are shown in figure 9. They were fabricated by the DEVCOM AC's Organic Materials and Prototyping Technology Branch using a FormLabs Form2 Desktop stereolithograph apparatus (SLA) machine in stock black resin. The machine uses photosensitive resin that is cured by a laser, which constructs the parts layer by layer with a support structure. The part was printed, cleaned with isopropyl alcohol, and post-cured in an ultraviolet (UV) oven. The support structure is manually removed, and a final wet sanding step is performed to smooth the part surface. Prototypes were assembled onto an Aerofuze Rev 3 fuze housing developed by DEVCOM AC, as shown in figures 10 and 11. This was later used for high-g shock survivability, in both the DEVCOM AC 155-mm air gun (surviving 12,000 g axial shock) and the DEVCOM AC SCATgun (surviving 10,000 g axial shock), with the unit successfully surviving both firings.

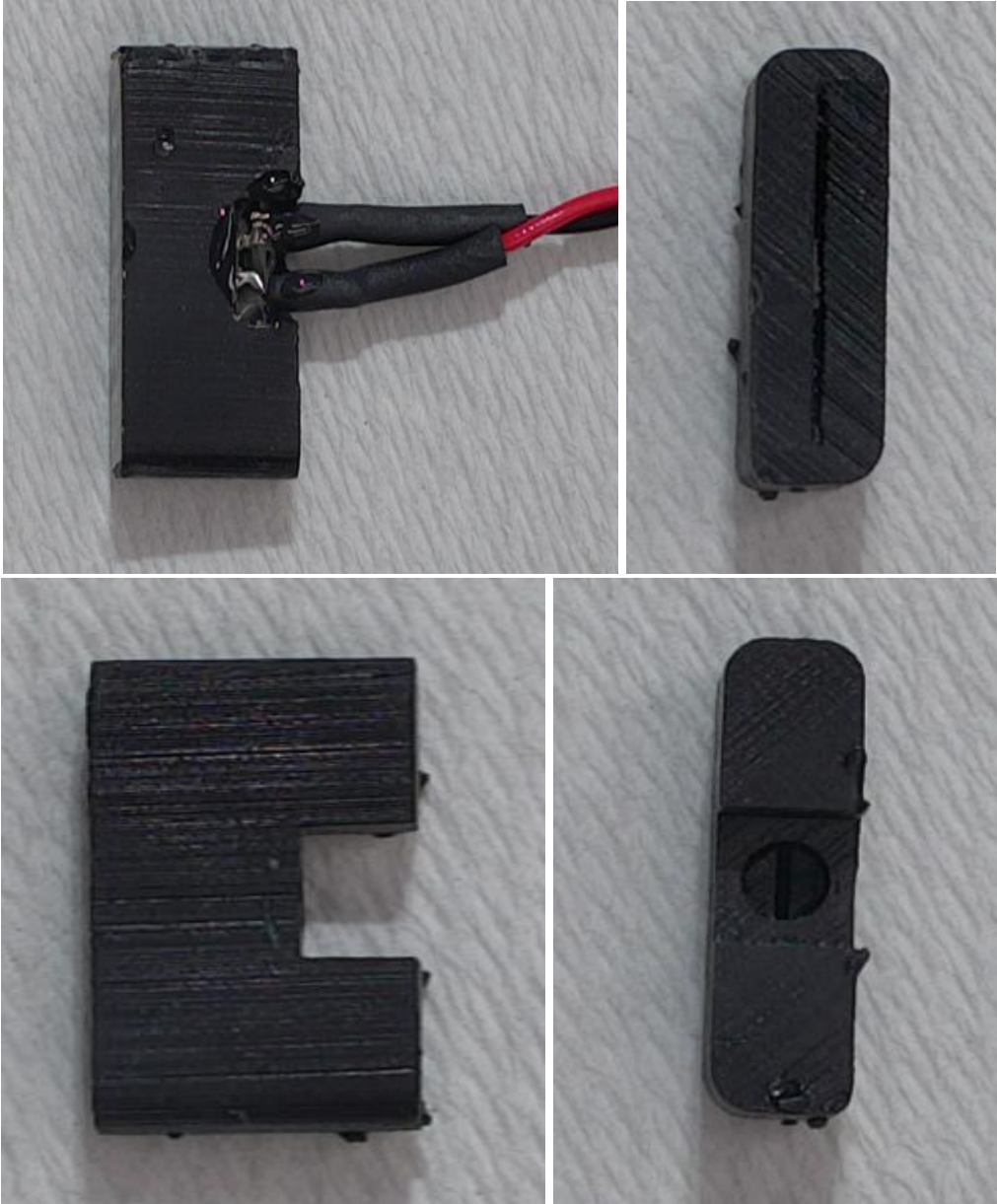


Figure 9
Plastic 3D-printed solar sensor

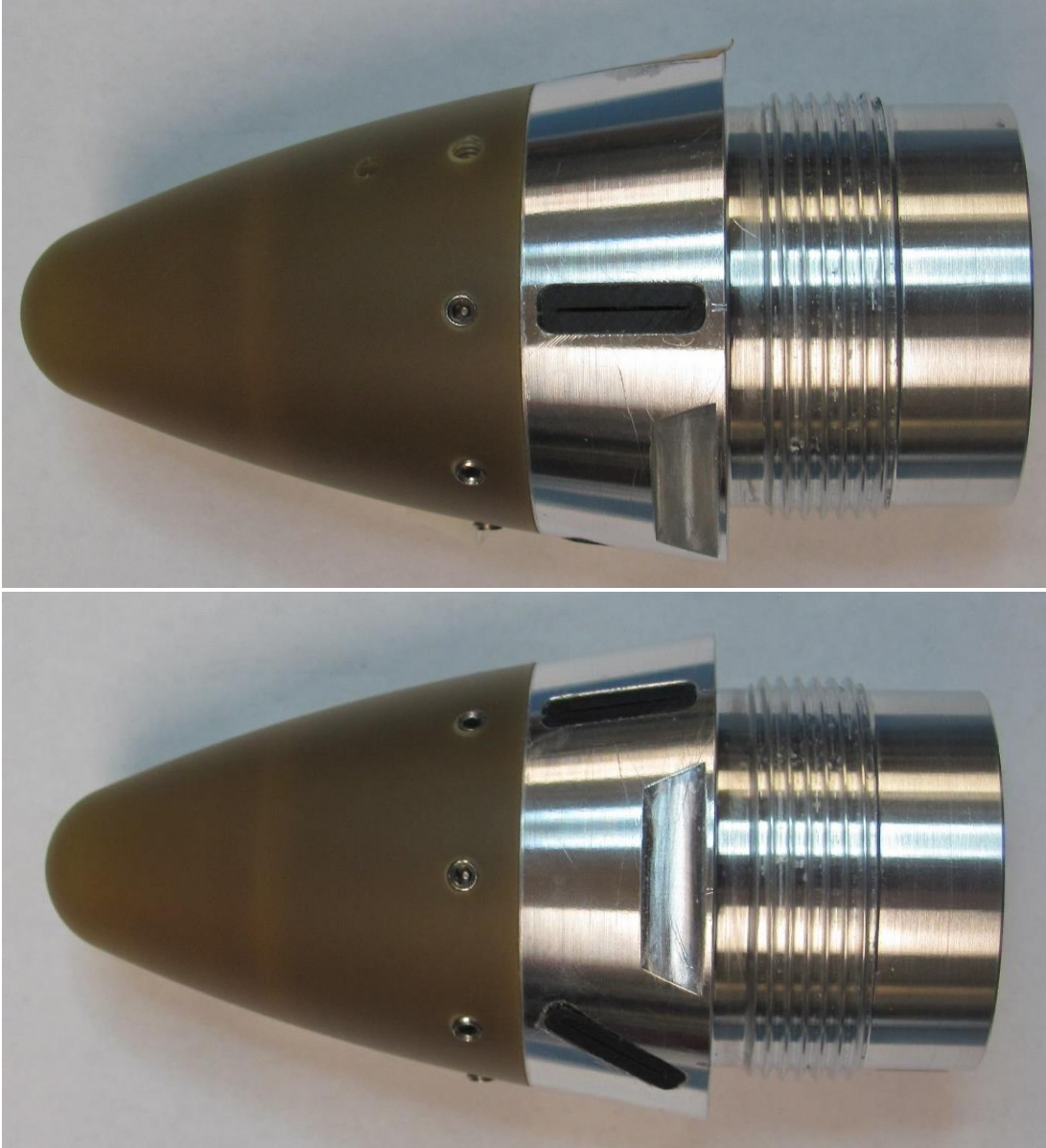


Figure 10
Plastic 3D-printed solar sensors mounted on fuze housing

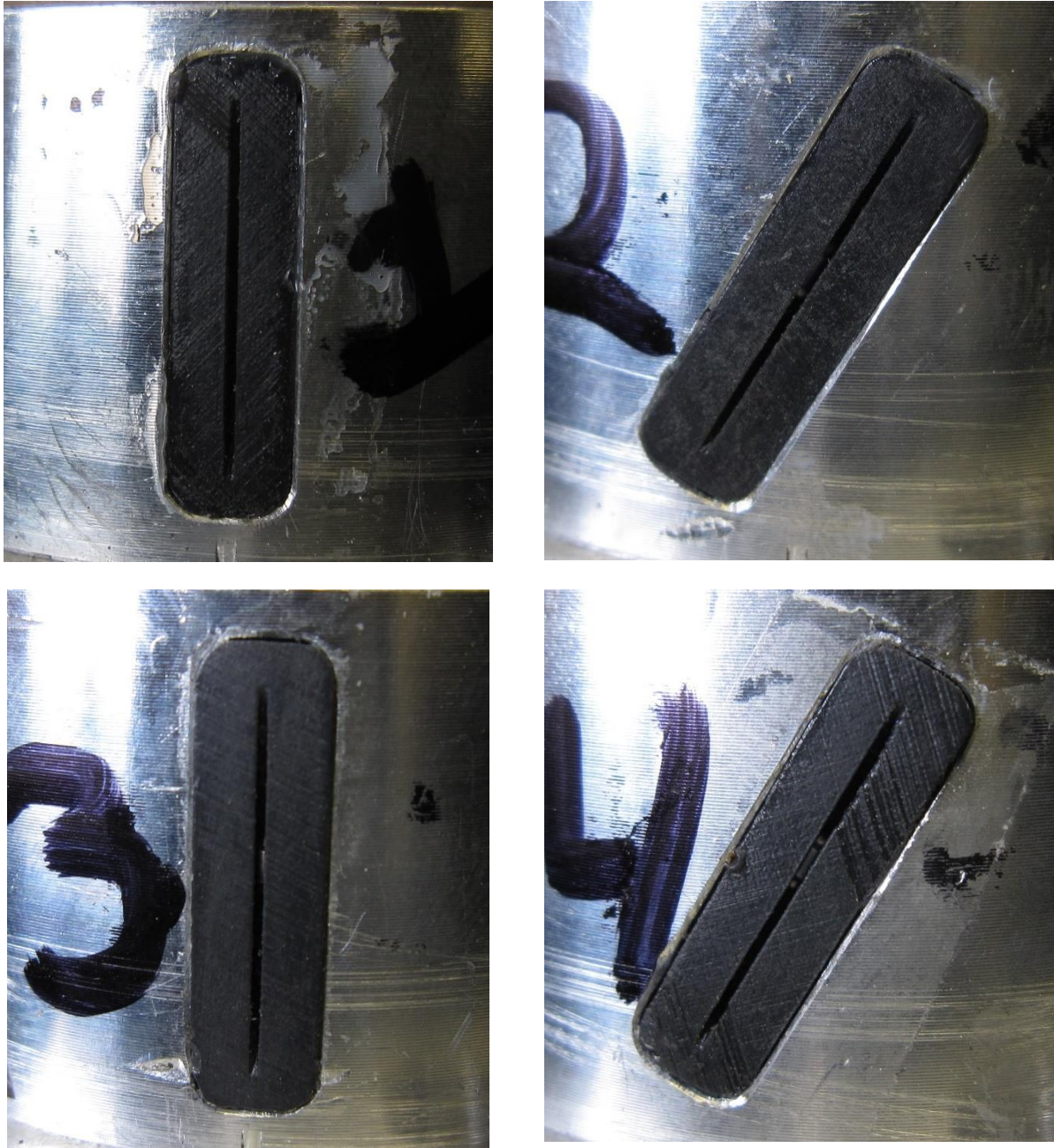


Figure 11
Plastic 3D-printed solar sensors mounted on fuze - up close view

The Prototyping and Powder Technology Branch at the DEVCOM AC additionally fabricated the sensor using an EOS M270 laser powder bed fusion machine. The sensors were built in 0.020-mm (20 μ m) layers out of in-house developed 4340 steel powder. After the sensors were fabricated, they were stress relieved and then removed from their build plate using electrical discharge machining. The parts are coated with black scale, which is a byproduct of the stress relieving process. The scale can be left on to keep the parts black, which is needed to absorb light and prevent reflections. The scale can be removed as shown in figure 12. However, the pieces will need to be coated again later with black material.

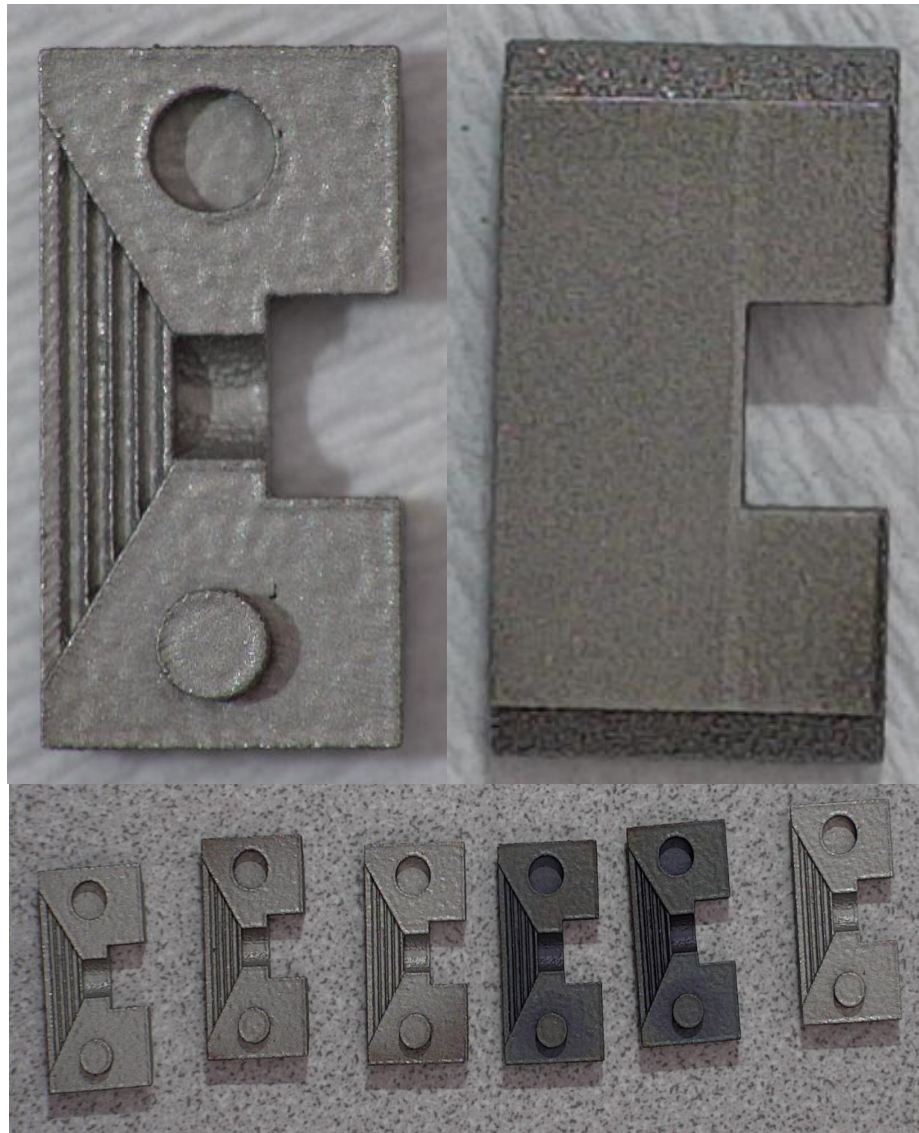


Figure 12
Two-piece metal clamshell 3D printed solar sensor with scale removed

Two versions of this sensor were made to address the gap width of the center slot: a one-piece sensor and a two-piece sensor. The first version was an attempt to produce a single piece sensor, as shown in figure 13. Multiple gap widths were attempted to get the 3D printing process correct. Eventually, metal parts were printed as a single piece with a well-defined slit of a 0.015 in. gap width. A comparison of the metal sensor and plastic sensor is shown in figure 14. For a finer slot width, the part was fabricated as a two-piece clamshell assembly, as shown in figure 15. This yielded a slot width of 0.005 in.

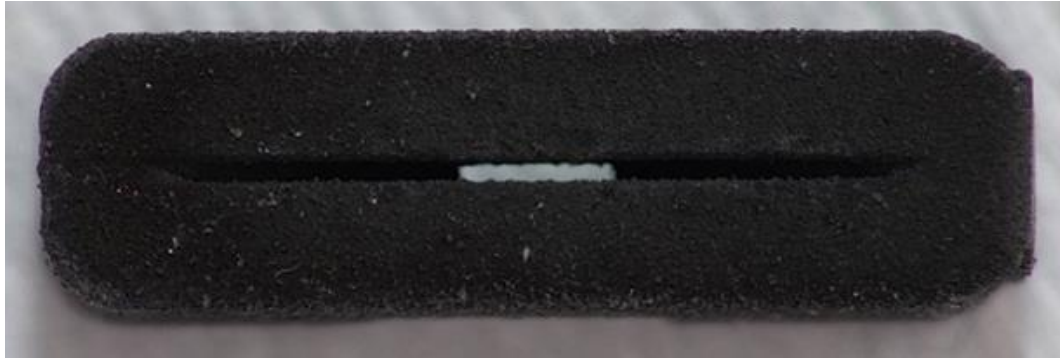


Figure 13

Single-piece metal (with scale) 3D-printed solar sensor: top - front/bottom - rear



Figure 14
3D-printed solar sensor slit comparison: top - single-piece metal with scale/bottom - single-piece plastic

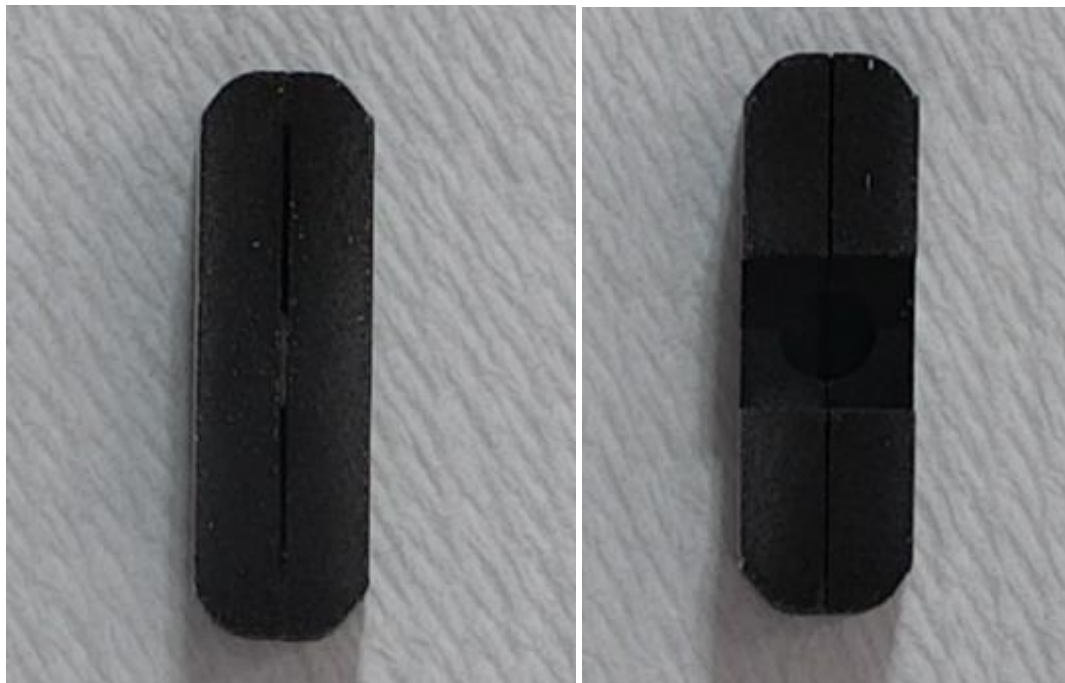


Figure 15
Two-piece scaled clamshell metal 3D-printed solar sensor

SENSOR OUTPUT COMPARISON

Several plastic 3D-printed solar sensors and ARL SLIT solar sensors were built onto ARRT-150 Aerofuze housings and placed onto a solar calibrator table, as shown in figure 16. Each fuze housing contained four sensors, two vertical, two tilted at 30 deg. The calibration table consists of a two-degrees of freedom motorized rotary table and a collimated halogen lamp acting as a sunlight simulator. The fuze housing fixture is first aligned with the principle axis of the lamp using a boresighted laser, then the fuze is screwed into the housing. The fuze housing is rotated through its roll angles and then stepped through yaw angles at 5-deg intervals. A National Instruments data acquisition system, interfaced with MATLAB, recorded the signal conditioned output of the photodiodes.



Figure 16
Solar sensor calibration table

The outputs of the solar sensors were signal conditioned using a printed circuit board containing the analog circuitry shown in figure 17. The schematic shows a pair of photodiodes (one vertical, one tiled) in photovoltaic mode, as a bridge configuration biased at 3 V. The input of the bridge is fed into an Analog Devices AD623 instrumentation amplifier, with a reference voltage set at 1.5 V. As light falls on one solar sensor, the voltage at its respective in-amp input falls, creating a pulse on the output. Two sets of sensors are combined with another instrumentation amplifier. This combines the outputs of all four solar sensors into a single analog channel.

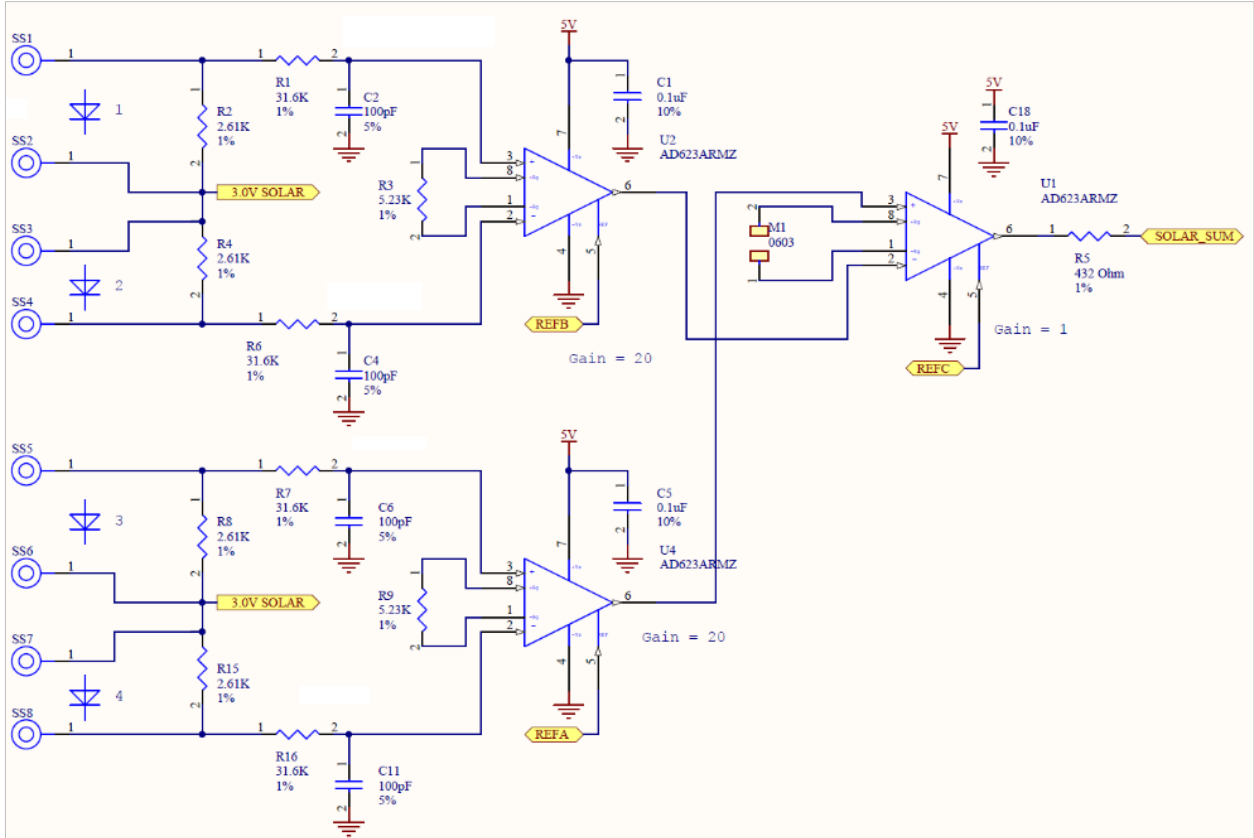


Figure 17

Schematic for solar sensor signal conditioning printed circuit board (P/N DEVCOM AC 0610-00424 AMM085-SS)

The output of the tilted sensors at yaw=80 deg (corresponding to sensor zenith) is shown in the plots in figure 18. The outputs are normalized to the maximum voltage measured. The plastic solar sensor saturates the signal conditioning, while the obstructors on the ARL sensor act to limit the signal to preserve a Gaussian shape. However, on one unit, the obstructor did not limit the signal causing the output to be saturated.

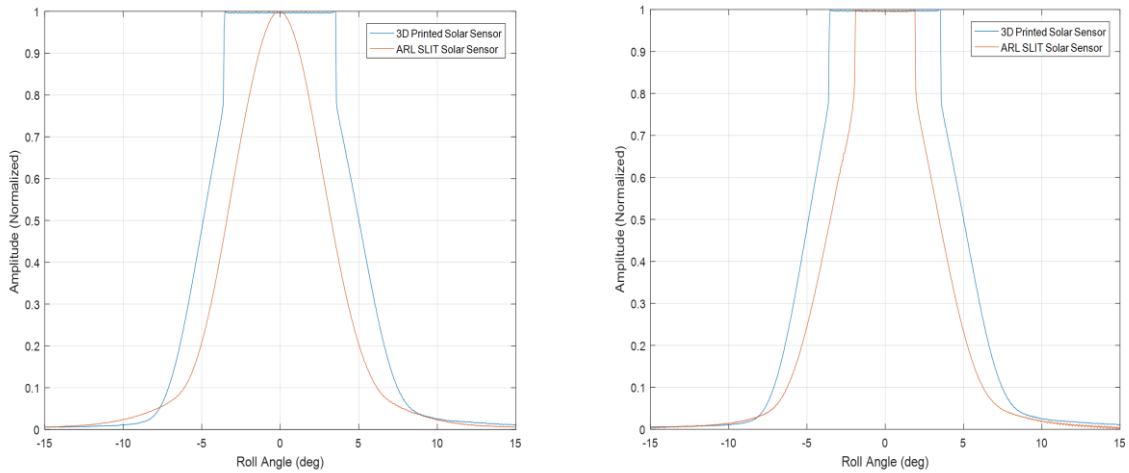


Figure 18
Comparison of plastic 3D solar sensor and ARL SLIT solar sensor signal outputs: left - unsaturated/right - saturated

The pulse width of the ARL sensor was measured as 10 deg (+/-5 deg) of roll angle (10.6 deg +/-5.3 deg for the saturated sensor) at the 0.2X reference level, which is more than the amount specified in reference 13 but agrees with plots shown in reference 20. The pulse width of the plastic solar sensor was slightly greater, 13 deg (-6.4/+6.6 deg) at 0.2 reference level with slight asymmetry observed. A discussion of the sampling rates required to digitize these signals can be found in reference 20.

The output of the tilted sensor over yaw for the plastic sensor is plotted in figure 19. In addition to the varying pulse position over yaw (the main sensor operation), the pulses quickly saturate the sensor between 50 and 110 deg of yaw. Signals are observed between 40 and 130 deg with no pulses observed beyond this range.

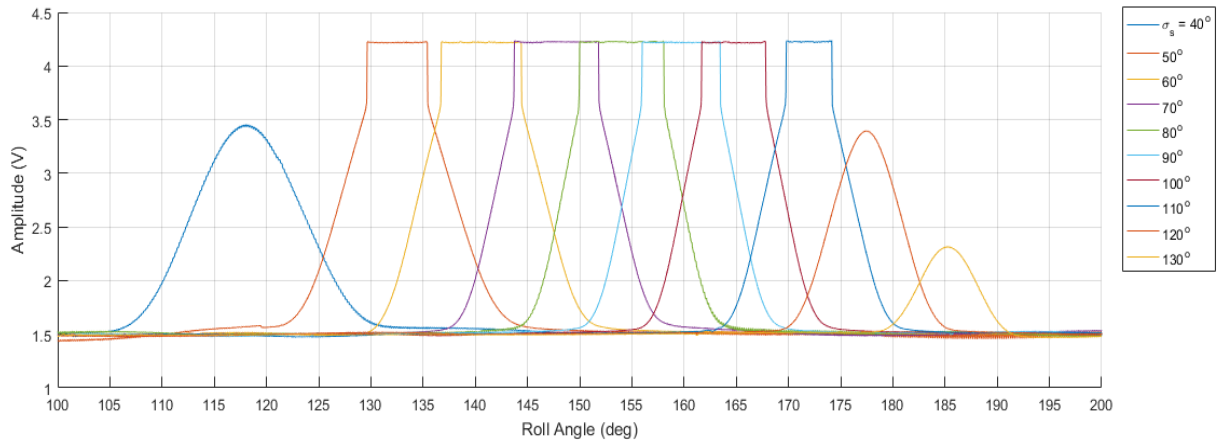


Figure 19
Plastic 3D-printed yawsonde output on a rotating fuze for solar aspect angles 40 to 130 deg

The output of the tilted ARL SLIT sensor is plotted in figure 20. The sensor range is greater as pulses are observed from 30 to 140 deg; however, the pulse widths elongate at the extremes. The pulses begin to merge into the pulses from the vertical sensor (off-axis on the left). Pulse height is generally limited by the obstructors; however, it is not uniform, and, at some angles (50 deg), the obstructors do not function.

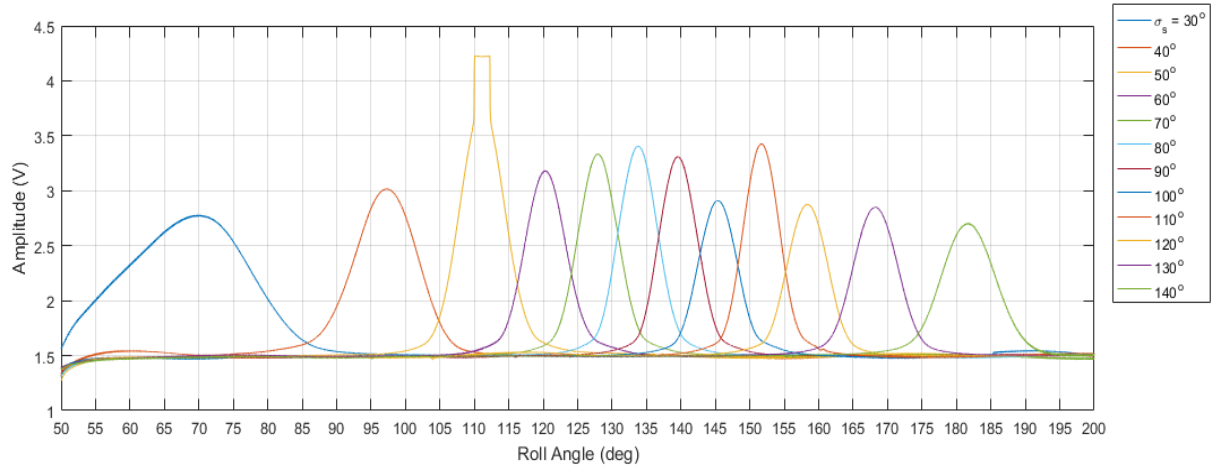


Figure 20
ARL SLIT sensor on a rotating fuze for solar aspect angles 30 to 140 deg

CONCLUSIONS

A three-dimensional (3D) printed solar sensor was developed, which is inexpensive to produce and easy to assemble. The sensor incorporates light-trapping ridge features printed directly into the housing, which previously needed to be machined into the sensor body. The sensor was fabricated in both metal and plastic. The sensor has a smaller field of view, and a wider pulse width than the current state-of-the-art U.S. Army Research Laboratory solar light indicating transducer solar sensor due to the lack of internal light reflectors and a wider aperture width. The performance of the 3D-printed solar sensors is still well suited for use in aeroballistics characterization of new projectile airframes. This design will enhance the instrumentation capability of future U.S. Army precision munitions programs by making solar sensors for yawsondes easier to produce and at a lower cost.

UNCLASSIFIED

REFERENCES

1. Hepner, D. and Harkins, T., "Determining Inertial Orientation of a Spinning Body With Body-Fixed Sensors," Technical Report ARL-TR-2313, U.S. Army Research Laboratory, Aberdeen Proving Ground, MD, January 2001.
2. Harkins, E. T., Davis, S. B., and Hepner, D. J., "Novel Onboard Sensor Systems for Making Angular Measurements on Spinning Projectiles," Proc. SPIE 4365, Acquisition, Tracking, and Pointing XV, doi: 10.1117/12.438045, 21 August 2001.
3. Decker, R., Davis, B., and Harkins, T., "Pitch and Yaw Trajectory Measurement Comparison Between Automated Video Analysis and Onboard Sensor Data Analysis Techniques," Technical Report ARL-TR-6576, U.S. Army Research Laboratory, Aberdeen Proving Ground, MD, September 2013.
4. Mermagen, W. H. and Clay, W. H., "The Design of a Second Generation Yawsonde," Memorandum Report BRL-MR- 2368, U.S. Army Ballistic Research Laboratory, Aberdeen Proving Ground, MD, April 1974.
5. Elmore, R., "HDL Yaw Sonde Instrumentation," Technical Manual HDL-TM-71-19, Harry Diamond Laboratories, Adelphi, MD, 1971.
6. Mermagen, W. H., "Measurements of the Dynamical Behavior of Projectiles Over Long Flight Paths," Journal of Spacecraft and Rockets, Vol. 8, No. 4, pp. 380-385, April 1971.
7. Ferguson, E. M., Hepner, D. J., and Clay, W. H., "Multisensor Pinhole Yawsonde," Technical Report ARL-TR-213, U.S. Army Research Laboratory, Aberdeen Proving Ground, MD, September 1993, <http://www.dtic.mil/get-tr-doc/pdf?AD=ADA271715>.
8. Ferguson, E. M. and Hepner, D. J., "Pinhole Yawsonde Sensor," International Telemetry Conference Proceedings, 1996.
9. Mermagen, W.H., "Projectile High-G Telemetry For Long Range Dynamics Measurements," Memorandum Report BRL-MR-2133, U.S. Army Ballistic Research Laboratory, Aberdeen Proving Ground, MD, October 1971.
10. Clay, W. H., "A Precision Yawsonde Calibration Technique," Memorandum Report BRL-MR-2263, U.S. Army Ballistic Research Laboratory, Aberdeen Proving Ground, MD, January 1973.
11. Gutler, E. and Gibbons, J., "Short Intrusion Yaw Sonde Development And Test Program," Laboratory Report TSI-D 1-76 (Unpublished), Instrumentation Division Technical Support Directorate, U.S. Army ARDEC, Picatinny Arsenal, NJ, October 1976.
12. Baroni, A. and Struck, J., "Yaw Sonde Capabilities," Laboratory Report (Unpublished), Commodity Evaluation Division Armament Engineering Directorate, U.S. ARDEC, Picatinny Arsenal, NJ.
13. Hepner, D. J., Hollis, M. S., and Mitchell, C. E., "Yawsonde Technology for the Jet Propulsion Laboratory (JPL) Free Flying Magnetometer (FFM Program)," Technical Report ARL-TR-1610, DTIC A352980, U.S. Army Research Laboratory, Aberdeen Proving Ground, MD, July 1 1998.

UNCLASSIFIED

REFERENCES

(continued)

14. Hepner, D. J., Hollis, M. S., Muller, P. C., Harkins, T. E., Borgen, G., D'Amico, W. P., Davis, B. S., and Burke, L. W., "Aeroballistic Diagnostic System," Patent US6349652B1, USPTO, Alexandria, VA, February 2002.
15. Davis, B., Harkins, T., Hepner, D., Patton, B., and Hall, R., "Aeroballistic Diagnostic Fuze (DFuze) Measurements for Projectile Development, Test, and Evaluation," Technical Report ARL-TR-3204, U.S. Army Research Laboratory, Aberdeen Proving Ground, MD, July 2004.
16. Hepner, D. J. and Hollis, M. S., "G-hardened optical alignment sensor," Patent US5909275A, USPTO, June 1, 1999.
17. Zuber, S., Hitscherich J., and Lansey, A., "Yawsonde Solar Sensor Assessment", Technical Report ARMET-TR-19003, U.S. Army DEVCOM AC, Picatinny Arsenal, NJ, In press.
18. Delgado, F. J., Quero, J. M., Garcia, J., Tarrida, C. L., Ortega, P. R., and Bermejo, S., "Accurate and Wide-Field-of-View MEMS-Based Sun Sensor for Industrial Applications," in *IEEE Transactions on Industrial Electronics*, vol. 59, no. 12, pp. 4871-4880, doi: 10.1109/TIE.2012.2188872, December 2012.
19. SolarMEMS Technologies, "Sun Sensor on a Chip Technical Specification, Interfaces & Operation," Specification Document SSOC-A60, November 2015.
20. Don, M. and Harkins, T., "Achieving High Resolution Measurements Within Limited Bandwidth Via Sensor Data Compression," Technical Report ARL-RP-444, U.S. Army Research Laboratory, Aberdeen Proving Ground, MD, June 2013.

UNCLASSIFIED

DISTRIBUTION LIST

U.S. Army DEVCOM AC
ATTN: FCDD-ACE-K
Picatinny Arsenal, NJ 07806-5000

Defense Technical Information Center (DTIC)
ATTN: Accessions Division
8725 John J. Kingman Road, Ste 0944
Fort Belvoir, VA 22060-6218

GIDEP Operations Center
P.O. Box 8000
Corona, CA 91718-8000
gidep@gidep.org

REVIEW AND APPROVAL OF ARDEC REPORTS

THIS IS A:

- TECHNICAL REPORT
- SPECIAL REPORT
- MEMORANDUM REPORT
- ARMAMENT GRADUATE SCHOOL REPORT

FUNDING SOURCE ARDEC S&T
 [e.g., TEX3; 6.1 (ILIR, FTAS); 6.2; 6.3; PM funded EMD; PM funded Production/ESIP; Other (please identify)]
 3D Printed Yawsode Solar Sensor

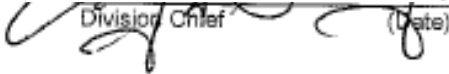
Title		Project
Aaron Barton		
Author/Project Engineer		Report number/Date received (to be completed by LCSD)
<u>x3521</u>	<u>95</u>	<u>RDAR-MEF-I</u>
Extension	Building	Author's Office Symbol

PART 1. Must be signed before the report can be edited.

- a. The draft copy of this report has been reviewed for technical accuracy and is approved for editing.
- b. Use Distribution Statement A , B , C , D , E , or F for the reason checked on the continuation of this form. Reason: _____
- 1. If Statement A is selected, the report will be released to the National Technical Information Service (NTIS) for sale to the general public. Only unclassified reports whose distribution is not limited or controlled in any way are released to NTIS.
- 2. If Statement B, C, D, E, or F is selected, the report will be released to the Defense Technical Information Center (DTIC) which will limit distribution according to the conditions indicated in the statement.
- c. The distribution list for this report has been reviewed for accuracy and completeness.

Craig Sandberg

20 DEC 2018


 Division Chief (Date)

PART 2. To be signed either when draft report is submitted or after review of reproduction copy.

This report is approved for publication.

Craig Sandberg

14 Jan 2021

Division Chief (Date)
 Arnold Klein
 RDAR-CIS 11/26/18 (Date)

LCSD 49 (1 Sept 16)
Supersedes SMCAR Form 49, 20 Dec 06